SURVIVABILITY ASSESSMENT AND LIFE-MODELING OF FINE PITCH SOLDER JOINT FUZE ELECTRONICS UNDER MECHANICAL SHOCK LOADS UP TO 50,000G

Pradeep Lall, Ph.D., Kalyan Dornala
Department of Mechanical Engineering
Auburn University
Auburn, AL, USA
lall@auburn.edu

Jason Foley, John Deep
Air Force Research Lab
Eglin, FL, USA

Ryan Lowe
ARA Associates
Littleton, CO, USA

ABSTRACT
Commercial electronics parts are increasingly being used in high-g fuzing applications. Sustainment of long-term systems requires the understanding of the survivability limits on newer fine pitch part architectures. In this study, the survivability of 0.4mm pitch and 0.5mm pitch parts at acceleration levels upto 50,000g have been studied for bare test boards, underfilled test boards, and potted test boards. In consumer electronics, survivability in mechanical shock is ascertained using the JEDEC JESD22-B111 test standard which involves the use of 1500g, 0.5ms shock pulse in a standard 132mm x 77mm, 15-parts test board. Consumer products may be designed in a number of form factors which may likely differ from the test board size and part configuration. Correlation of performance in JEDEC test to actual product performance is often weak. In order to alleviate this limitation of the JEDEC test, the test assembly in the present study has been designed in the form factor of the actual use application to be circular with an annular ring in the center. Two categories of underfills has been used including Lord Thermoset ME-531, and Loctite UF 3811. Two categories of potting compounds have been used including Armstrong A12, Henkel Stycast 2850FT. Armstrong A12 is a low modulus material and Henkel Stycast 2850FT is a high modulus material intended for shock applications. Digital image correlation has been used to measure the strain field of the board assembly during impact. Failure of interconnects has been detected using a high-speed data acquisition system. The transient dynamic motion of the board assemblies and the strains in interconnects have been modeled using ABAQUS Explicit finite element models.

INTRODUCTION
Electronics in aerospace and missile applications may be subjected to high-acceleration levels during normal operation. Missile applications increasingly use commercial-off the shelf electronics components with the expectation of reliable operation under acceleration loads up to 50,000g. Military systems differ from the consumer electronics counterparts in the expected lifetimes and expected reliability. Newest electronics technologies find their way into consumer applications much before their introduction into high-rel applications such as aerospace and missile platforms. The primary reason is risk-averseness towards the use of technologies which often push the edge of the envelope in terms of miniaturization and in many cases, cannot be compared with the state-of-art systems in operation and lack decades of historical data to provide robust proof of their survivability. Tools and techniques are needed to determine the failure envelopes for new component technologies which were originally designed for office benign applications, under high acceleration loads in current and next generation military systems. The JEDEC JESD22-B111 test standard is often used for consumer electronics for the assessment of the mechanical shock survivability of electronics components. The components are arranged in a 3 x 5 array on a board with dimensions of 132mm x 77mm and subjected to a 1500g, 0.5ms pulse [JEDEC 2003]. The correlation of the test results with the survivability of the components in the product is quite weak. The reason for the poor correlation is that the component's survivability in the product configuration is influenced by many additional factors including shock orientation, board material, number of layers, product size, board thickness, component location, proximity of the component to the external housing, and component design rules. The same component may have large difference in shock survivability depending on the product implementation.

In this study, the shock-survivability of the components in the end application has been assessed using a circular test

board which is representative of the end application in the projectile. High strain rate survivability of electronics has been studied by previous researchers including the measurement of deformation and strain in board assemblies subjected to shock loads [Lall 2005, 2007, 2008, 2012; Tian 2005]. Digital image correlation has been applied to the field of semiconductor packaging for acquisition of solder joint deformation under thermal loading by [Xu 2006, Yogel 2001, Zhou 2001, Zhang 2005]. Deformation fields in transient dynamic loads such as mechanical shock may not often be symmetrically applied to interconnect in the components. In addition, the location of the peak strain or displacement may not be known a-priori making it difficult to select the location of the strain gage on the printed circuit board assembly. The use of digital image correlation in conjunction with high-speed imaging provides the advantage of full-field strain acquisition in the assembly without any a-priori knowledge of the anticipated deformation field or locations of peak strain in the interconnects. A circular test board with annular ring has been used for the experimental assessment of survivability. The board has an outer diameter of 110mm and the annular ring diameter of 36mm. The survivability of three board configurations has been studied including unreinforced component board assemblies, underfilled board assemblies, and potted board assemblies. Each of the board assemblies has been subjected to three mechanical shock conditions of increasing severity including 10,000g, 0.2ms shock pulse; 25,000g, 0.08ms shock pulse, and 50,000g 0.07ms shock pulse. In each case, explicit finite element models of the board assemblies have been created to simulate the mechanical shock event and predict the strain histories in the solder joint interconnects. Two high-speed cameras have been used to capture the out-of-place deformation of the board assembly, which had been previously been speckle coated. All the parts on the test assemblies are daisy chained. Failure of the parts has been detected using a high-speed data-acquisition system. While fine pitch electronics components with interconnect-pitch in the neighborhood of 0.4mm have been used in consumer electronics applications, relatively little is known about the survivability of 0.4mm pitch components under mechanical shock loads of 50,000g. Furthermore, the ability of enhancing design margins using underfills, and potting compounds at high-g loads is also relatively unknown. It is this void in the state-of-art that the present work intends to address.

TEST VEHICLE

The test matrix of components consists of two 0.4mm pitch packages including the CVBGA97, CVBGA360, and three 0.5mm pitch packages including the CTBGA84, CTBAG132 and CTBGA228. All the test packages are located on the same test board axially distributed along the circumference of the test board. The board assembly has been designed to mimic the actual test board by using an 8-layer construction, and inclusion of cross-hatched copper pattern on the internal layers to capture the effect of copper loading.

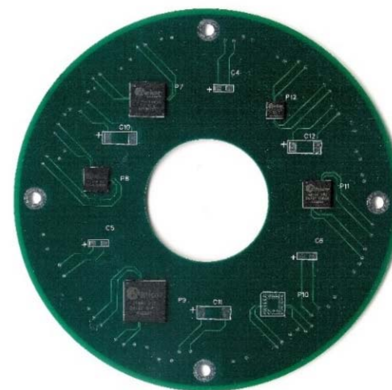

Figure 1: Test Vehicle-Packages with no reinforcement (Unreinforced Test Vehicle)

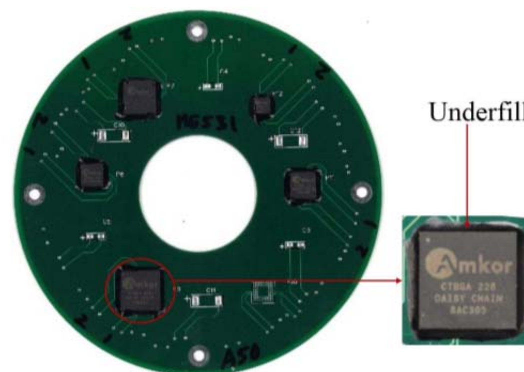

Figure 2: Test Vehicle- Packages reinforced with Lord Thermoset ME531 underfill

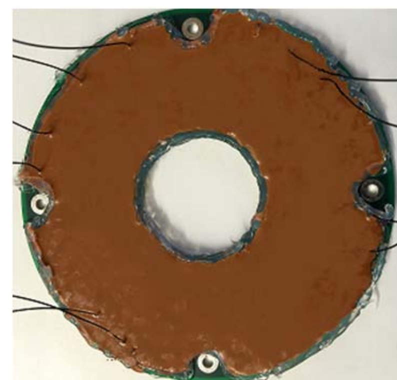

Figure 3: Test Vehicle- Armstrong A12 potted and underfilled

Furthermore, the test assemblies have been studied in three configurations including unreinforced, underfilled and potted assemblies. The BGA packages are placed on the board such a way that they are angularly spaced from each other and symmetrically located with respect to edges of the board. The test vehicle had two levels of package reinforcements. First configuration includes the Lord Thermoset ME531 underfill reinforced packages and the second configuration includes epoxy potting the PCBs with underfilled packages. Two categories of potting compounds have been used including Armstrong A12, Henkel

STYCAST 2850FT. Armstrong A12 is a low modulus material and Henkel STYCAST 2850FT is a high modulus material intended for shock applications.

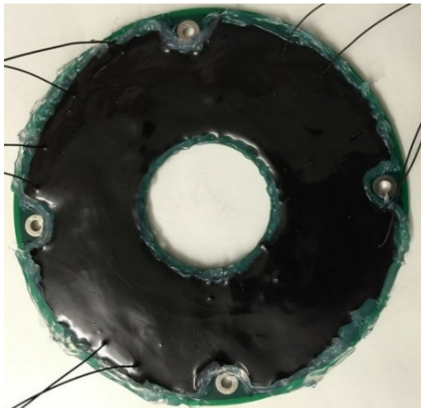

Figure 4: Test Vehicle-STYCAST 2850FT potted and underfilled

Table 1: Package Attributes for 0.5mm Pitch Packages

Package Attributes			
Package	CTBGA84	CTBGA132	CTBGA228
Location on board	P8	P11	P9
Body Size	7mm	8mm	12mm
I/O Count	84	132	228
Ball Pitch	0.5mm	0.5mm	0.5mm
Matrix	12 x 12 Perimeter	14 x 14 Perimeter	22 x 22 Perimeter
Ball Diameter	0.3mm	0.3mm	0.3mm
Substrate Pad	NSMD (Board) SMD (Package)	NSMD(Board) SMD(Package)	NSMD (Board) SMD (Package)

Table 2: Package Attributes for 0.4mm Pitch Packages

Package Attributes		
Package	CVBGA360	CVBGA97
Location on board	P7	P12
Body Size	10mm	5mm
I/O Count	360	97
Ball Pitch	0.4mm	0.4mm
Matrix	23 x 23 Perimeter	10 x 10 Full Array
Ball Diameter	0.25mm	0.25mm
Substrate Pad	NSMD (Board) SMD (Package)	NSMD(Board) SMD(Package)

The PCB surface was cleaned thoroughly with rubbing alcohol and the potting compound mixture was poured on to the annular well of the board leaving the space for standoffs. The potting material is roughly two times of the height of the packages and is cured at room temperature for 24 hours. Both potting compounds have a similar glass transition temperature in the neighborhood of 60°C. Figure 1 shows the bare test assembly without the use of any underfill or potting compound. Figure 2 shows the test vehicle with ME531 underfill reinforced packages. Figure 3 and Figure 4 show the PCBs that have been potted with epoxies Armstrong A12 and STYCAST 2850FT respectively. Both the Armstrong A12 and STYCAST 2850FT potted board assemblies have been pre-reinforced with ME531 underfill beneath the packages before potting. Semiconductor package attributes for all the packages on the test assembly are shown in Table 1 and Table 2.

EXPERIMENTAL SET-UP

A. Drop Test

The circular test assembly (Figure 5) was setup on the drop tower and connected to a continuity board for event detection of opens in the test assembly during the shock event. The continuity board was connected to a data-acquisition board for recording of the events during the shock event. In addition, acceleration pulse during the shock event was recorded from the shock-table through a signal conditioning unit. Pulse-shapers were used to procure the needed pulse width of the shock pulse. Bare, underfilled, and potted board assemblies were subjected to shock pulses at 10,000g for 0.2ms; 25,000g for 0.08ms; and 50,000g for 0.07ms shock levels. The high-g levels in excess of 5000g have been attained using a dual mass shock amplifier on the shock table of the drop tower. The mechanical shock pulse during the shock event was recorded using an accelerometer with a sensitivity of 0.103mV/g. All the packages on the test board are daisy-chained and were monitored for failure during mechanical shock event using high-speed data acquisition. Two high-speed video cameras were used to capture the deformation of the board assembly during mechanical shock. Drop heights for each g-level were found experimentally. The drop height for 10,000g was 38.5inches; for 25,000g was 52.6inches, and for 50,000g levels was 62.4 inches. All packages were monitored in-situ for continuity using high speed data acquisition system. In order to measure the full field strain and displacement of the test board 3D DIC has been performed. The test boards were speckle coated and the transient dynamic shock event was captured using high speed camera at 8,000fps. Figure 6, Figure 7, and Figure 8 show the reference shock pulses from the accelerometer for 10,000g, 25,000g and 50,000g respectively.

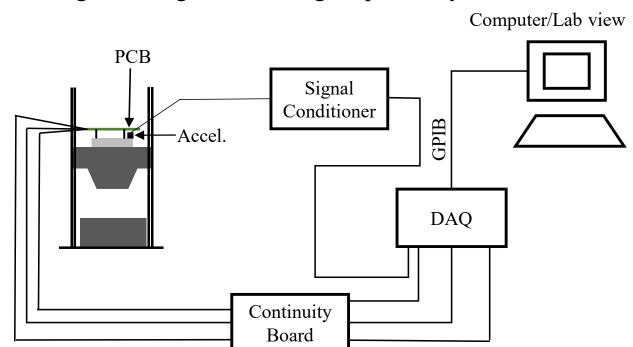

Figure 5: Drop Test Layout

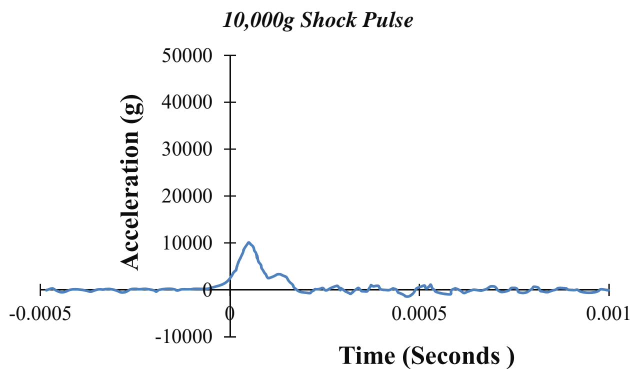

Figure 6: 10,000g shock pluse

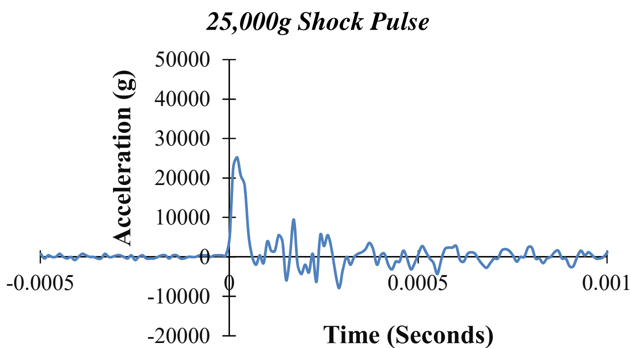

Figure 7: 25,000g shock pulse

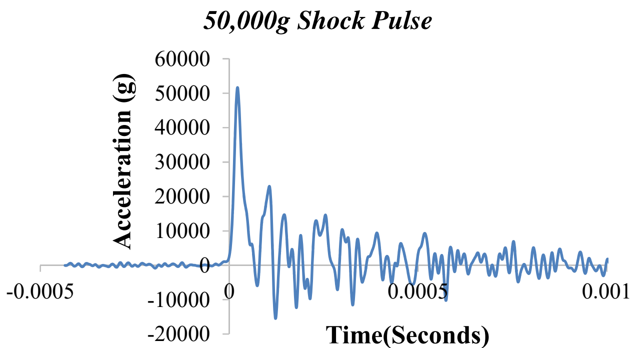

Figure 8: 50,000g shock pulse

B. 3D-DIC

Board assembly strains during the shock event were measured using digital image correlation. A random speckle pattern was applied to the visible surface of the test board closest to the high-speed camera. Motion of the speckles was measured using correlation functions and the gradient of the deformation were used to calculate the strain field. Transient dynamic motion has been captured using a frame rate of 8,000 fps in order to capture the full-field of motion of the board assembly. The cameras have been mounted on rigid tripod supports close to the shock tower. The cameras have been constrained to prevent any movement of the camera during the shock event relative to the shock tower or relative to each other. The high-speed video captured during the shock event has been used extract images for measurement of displacement and strain using VIC-3D DIC software. The ability to capture strains accurately using digital image correlation has been previously demonstrated using comparison of the acquired strain signal from digital image correlation with the strain signal from strain gage [Lall 2007, 2008, 2012]. The board assembly without strain has been imaged to capture the reference image. The reference image has been used to establish the floor from which all the deformations and strains have been measured. The deformation has been measured by tracking the speckle pattern on the printed circuit board. Each speckle pixel has been identified using the pattern formed by the speckle and its nearest neighbors in the subset. The correlation of the pattern formed by the speckle of interest and its nearest neighbors in the subset has been computed for each of the frames in the high-speed event. A high value of the correlation allows the identification of the speckle pattern's position and motion during the transient dynamic event. In order to enable the ability for identification of the pattern of motion, the speckle pattern used is random in nature. The subset of pixels has been stepped through the image to allow for computation of the displacement pattern in the board assembly. Cross-correlation function has been used for computation of the correlation between the reference and the deformed images.

ABAQUS EXPLICIT FINITE ELEMENT MODELING

The transient dynamic motion of the printed circuit board assembly during the high-g shock event has been modeled with explicit finite element model developed in ABAQUS explicit.

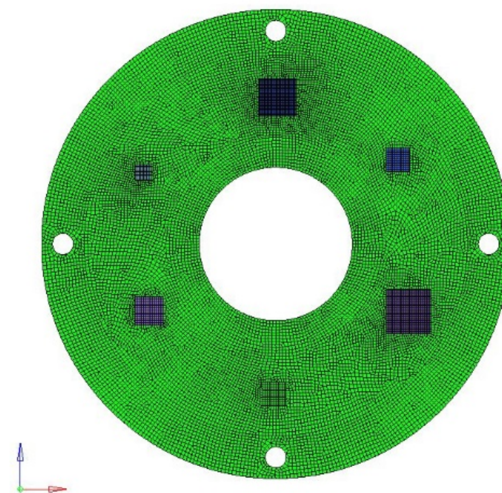

Figure 9: Explicit Finite element model in ABAQUS Explicit for an unreinforced printed circuit board assembly.

The model has been developed for all the three configurations of the board assembly including unreinforced, underfilled, and potted. The PCB in the assembly was modeled with reduced integration shell elements called S4R elements, while the remaining package elements including the electronic mold compound, chip, die-attach, organic substrate, underfill, and potting compound were modeled with 3D reduced integration continuum

elements called C3D8R elements. All interconnects in the semiconductor packages have been modeled using 3D Timoshenko-beam elements called B31 elements.

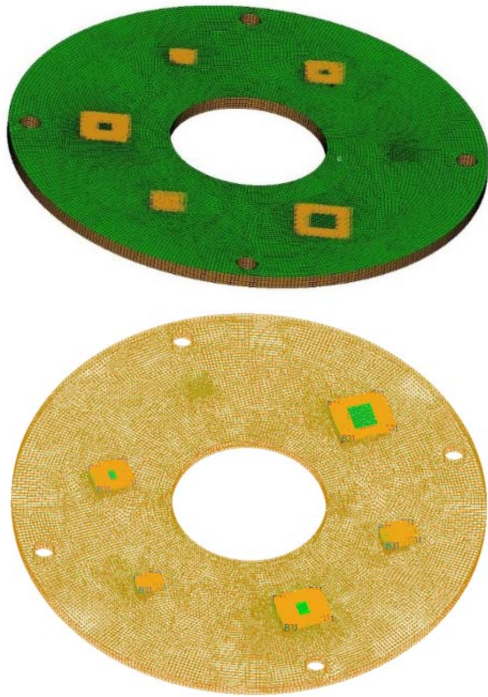

Figure 10: Printed Circuit Board Assembly reinforced with Epoxy potting compound.

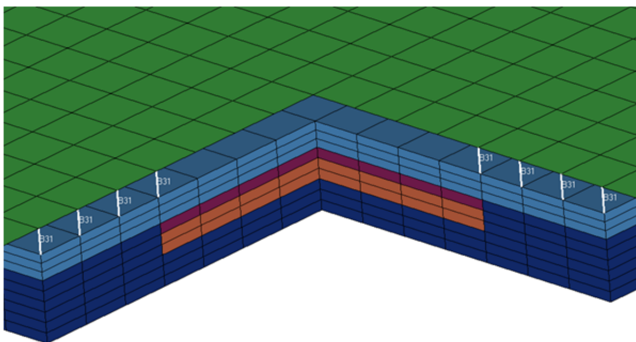

Figure 11: Unreinforced package

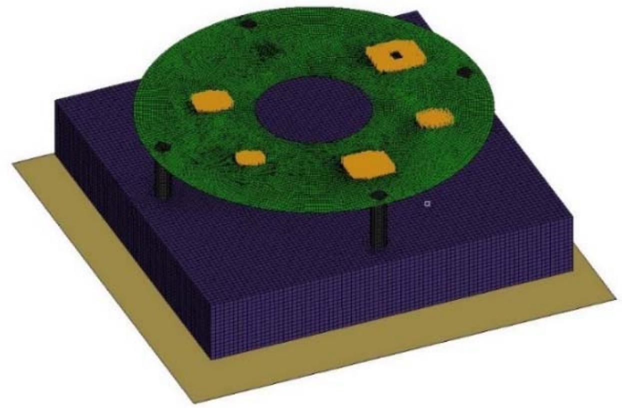

Figure 12: Transient dynamic shock model including drop base and rigid floor.

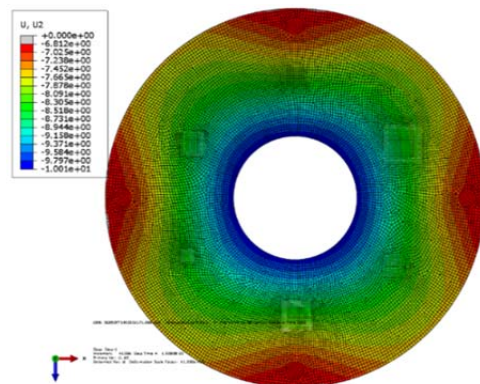

Figure 13: STYCAST 2850FT potted TV model displacement @ 10,000g shock

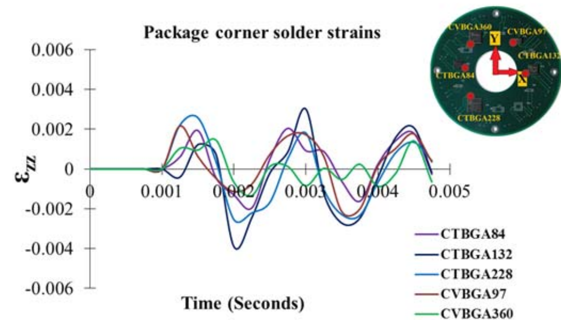

Figure 14: Corner solder interconnect strains of STYCAST 2850FT epoxy potted board @ 10,000g

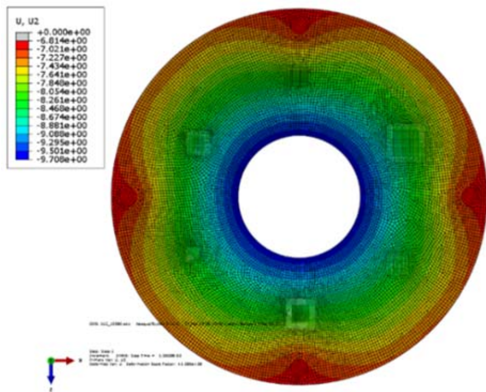

Figure 15: Armstrong A12 potted TV model displacement @ 10,000g shock

An unreinforced test assembly model is shown in Figure 9. Epoxy potted test vehicle model is shown in Figure 10. A zoomed-in view of the model of an unreinforced package on the test assembly is shown in Figure 11. The board assembly mounted in the configuration of the drop test on the drop tower is shown Figure 12. The floor for drop-simulation shown in Figure 12 has been modeled as a rigid floor using 3D rigid 4-node elements called R3D4 elements. In order to detect contact of the test assembly with the rigid floor, node-to-surface contact has been used and a reference node has been placed behind the rigid floor in the simulation. While the complete drop-event is a few milliseconds long, the highest strain amplitudes are encountered during the first few milliseconds of the impact accompanied with damage to the assembly interconnects and interfaces. It is for this reason that the modeled length of the shock event has been limited to 5ms after impact. In order to allow for a sufficient resolution of the time-history obtained from the simulation, the data on deformation and strain has been output at an interval of 0.1ms.

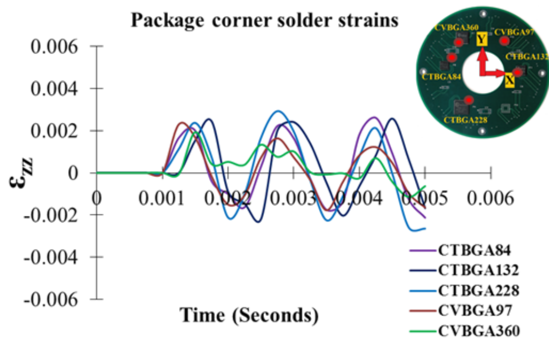

Figure 16: Corner solder interconnect strains of Armstrong A12 potted board @ 10,000g

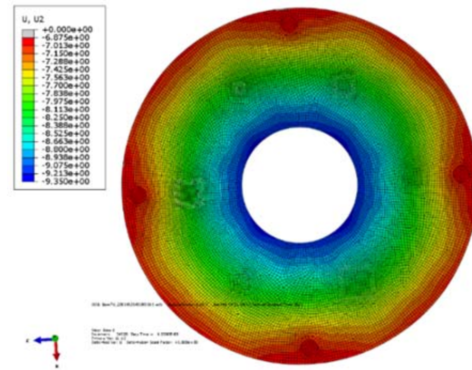

Figure 17: Unreinforced bare TV displacement @ 25,000g shock

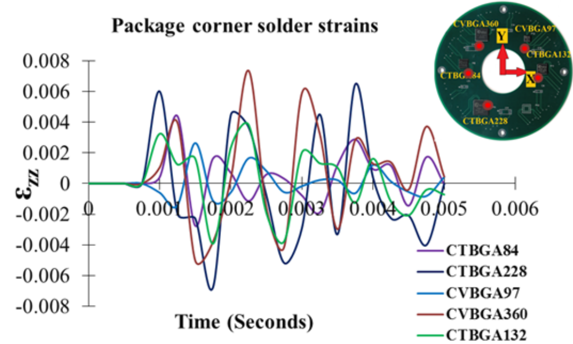

Figure 18: Corner solder interconnect strains of bare TV @ 25,000g

Peak displacement contour predictions from model predictions of the transient-dynamic shock event have been extracted for all the configurations of the board assemblies. Board strains have been studied in addition to interconnect strains during the impact. In each case, the solder joint strains have been extracted for the time-step with the peak out-of-plane board displacement. Figure 13 and Figure 14 show the out-of-plane deflection and corner solder-joint strain respectively for the STYCAST 2850FT potted TV under 10,000g. The location of the corner solder-joint where the peak solder strain were exhibited are shown by the red dots in the plot. The peak FE displacement for 10,000g STYCAST 2850FT potted board is 2.52mm and peak solder strain is 3900με for the package CTBGA132. Figure 15 and Figure 16 show the out of plane deflection contour and the corner solder interconnect strains of Armstrong A12 potted board under 10,000g. Peak FE displacement is 2.49mm and the peak corner solder strain is 2900με.

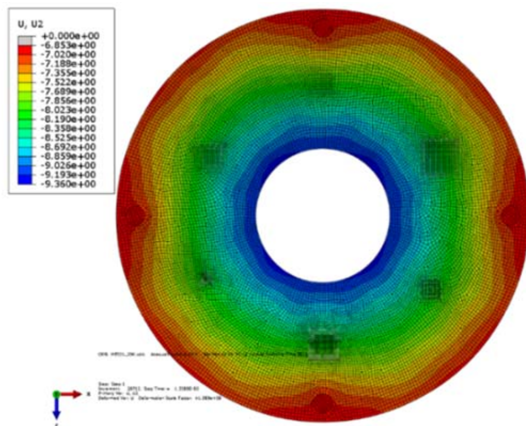

Figure 19: ME531 underfill reinforced TV displacement @ 25,000g shock

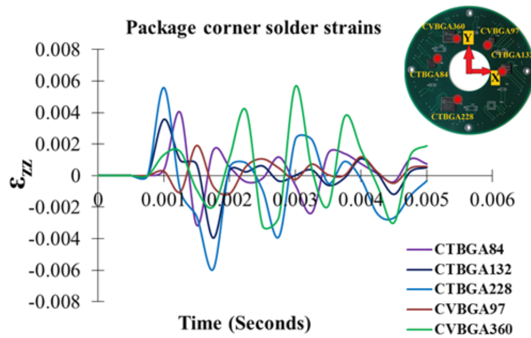

Figure 20: Corner solder interconnect strains of ME531 underfill reinforced TV @ 25,000g

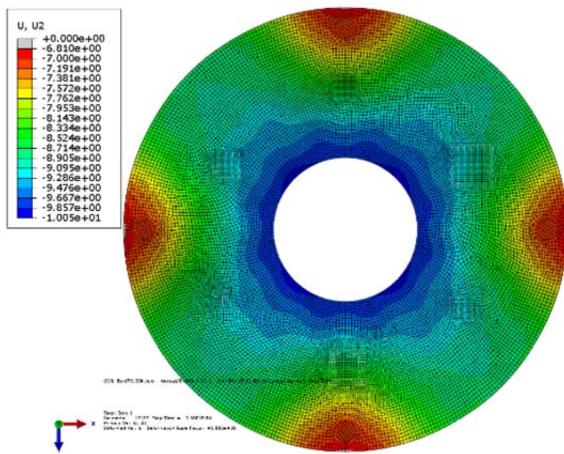

Figure 21: Unreinforced bare TV displacement @ 50,000g shock

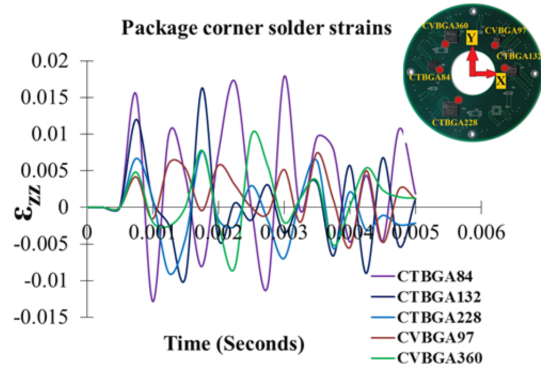

Figure 22: Corner solder interconnect strains of Bare TV @ 50,000g shock

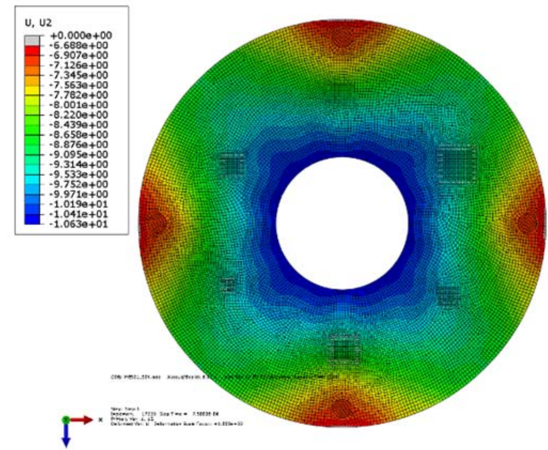

Figure 23: ME531 underfill reinforced TV displacement @ 50,000g shock

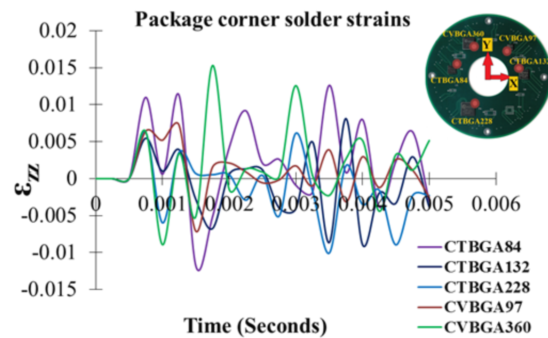

Figure 24: Corner solder interconnect strains of ME531 underfill reinforced TV @ 50,000g

From the model predictions of 25,000g shock displacement contours and corner solder strains were extracted from the explicit dynamic analysis. Figure 17 and Figure 18 show the displacement contours and the corner solder interconnect strains of unreinforced bare package TV subjected to 25,000g shock. Peak displacement value at the center is 2.69mm and the peak solder interconnect strain is 6400με. The displacement contour just after the impact and the corner solder interconnect strains for the ME531 underfilled TV at 25,000g shock are shown in Figure 19 and Figure 20

respectively. Peak displacement value is 2.54mm and the peak corner solder interconnect strain is 5900με. In comparison with the values at 10,000g, the peak displacements at the 25,000g shock level for both the unreinforced and the underfilled configurations show an increase of about 0.2mm and the peak solder strains also follow this trend by a change of 2500-3000με. The out of plane board displacement and solder interconnect strains of unreinforced bare TV at 50,000g shock are shown in Figure 21 and Figure 22 respectively. Peak displacement for the 50,000g test condition is 3.29mm and the maximum solder interconnect strain value is seen for the package CTBGA84 with a peak strain value of 15200με. In Figure 23 and Figure 24 the out of plane displacement after the impact and the solder interconnect strains in the package corner for ME531 underfill reinforced TV at 50,000g shock are shown respectively. The peak displacement value from the contour is 3.18mm and the peak solder interconnect strain is seen in CVBGA360 with peak strain values of 14800με.

HIGH-G SHOCK SURVIVABILITY TESTS

The deformation history captured using high-speed imaging has been used to measure the board deformation and strain at specific locations with high-propensity for damage. Package corners have high propensity for damage to interconnect under mechanical shock.

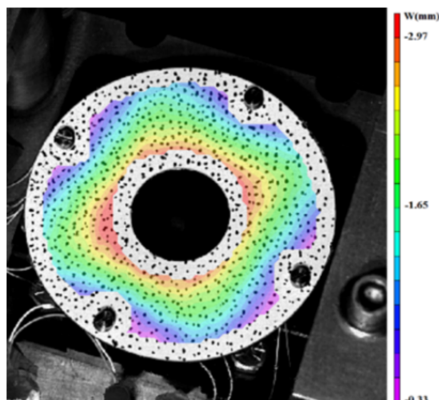

Figure 25: Out-of-Plane Displacement for Test Assembly with Epoxy 2850FT @10,000g

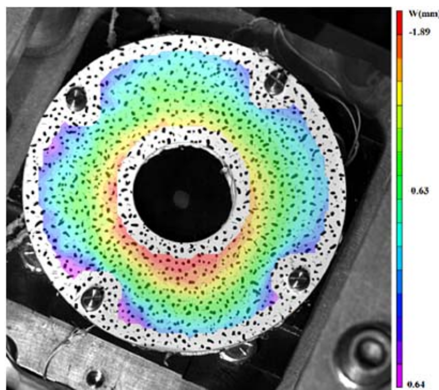

Figure 26: Out-of-Plane Displacement for Test Assembly with Epoxy Armstrong A12 @ 10,000g

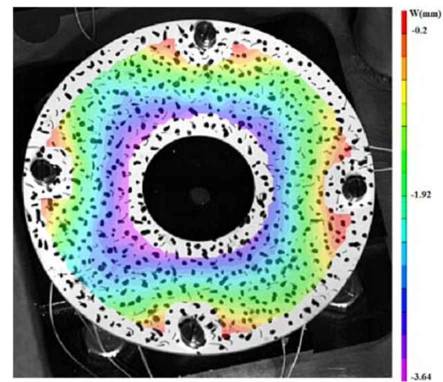

Figure 27: Out-of-Plane Displacement for Unreinforced Test Assembly @ 25,000g

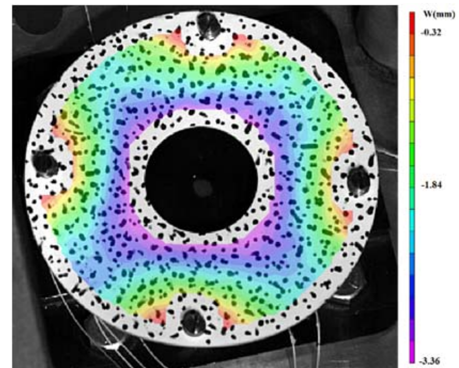

Figure 28: Out-of-Plane Displacement for Test Assembly with ME531 underfill @ 25,000g

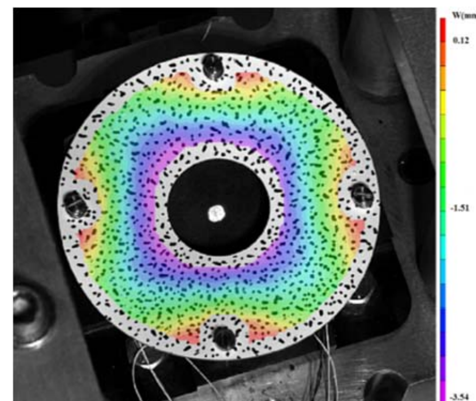

Figure 29: Out-of-Plane Displacement for Unreinforced Test Assembly with @50,000g

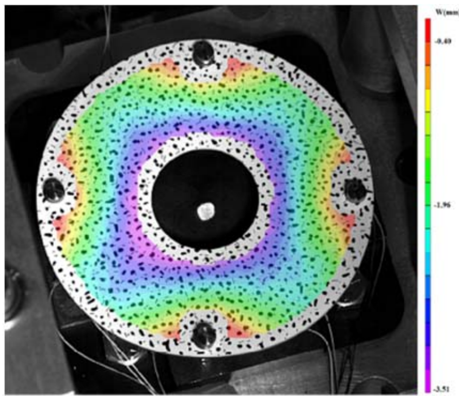

Figure 30: Out-of-Plane Displacement for Test Assembly with ME531 underfill @ 50,000g

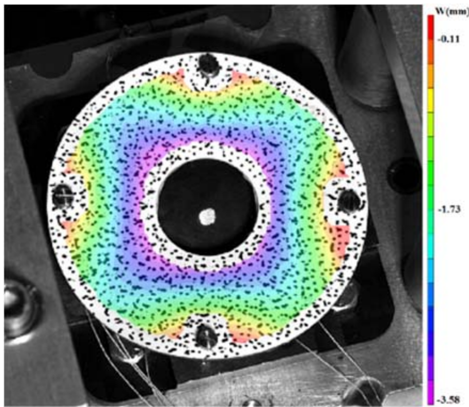

Figure 31: Out-of-Plane Displacement for Test Assembly with Armstrong A12 @50,000g

The displacement contours shown this section were the peak deflection contours just after the impact. Figure 25 shows the DIC measurements shows the out-of-plane displacement contours for STYCAST 2850FT epoxy potted board at 10,000g shock event. The measured peak displacement near the center was 2.59mm. Out of plane displacement contours for Armstrong A12 potted test board subjected to 10,000g shock are shown in Figure 26. The peak displacement with Armstrong A12 potting compound is exhibited near the center with a peak value of 2.48mm. Figure 27 and Figure 28 show the displacement contours for the 25,000g shock event of bare unreinforced TV and ME531 underfill reinforced TV respectively. The peak values corresponding to the bare TV and ME531 underfill TV at 25,000g are 3.41mm and 3.08mm. Figure 29 and Figure 31 show the displacement contours from 50,000g transient dynamic shock event. Peak displacement for unreinforced bare TV @50,000g is 3.62mm shown in Figure 29. The peak displacements for ME531 underfill reinforced and Armstrong A12 epoxy potted TVs shown in Figure 30 and Figure 31 are 3.19mm and 3.39mm respectively. The test board with STYCAST 2850FT epoxy failed at the 2nd drop and potting material delaminated at 1st drop itself under 50,000g.

PCB Strains

In addition to displacement contours, the board strains in the vicinity of the corner interconnects have been extracted from DIC Analysis.

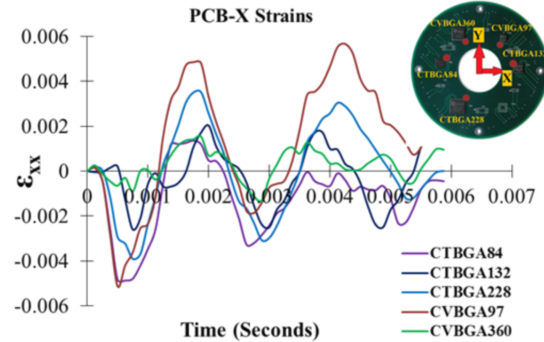

Figure 32: PCB-X strains of STYCAST 2850FT potted board @ 10,000g

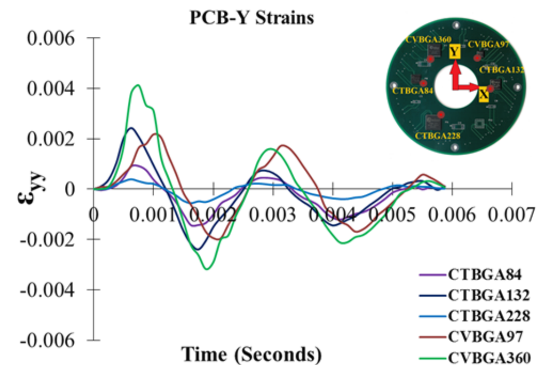

Figure 33: PCB-Y strains of STYCAST 2850FT potted board @ 10,000g

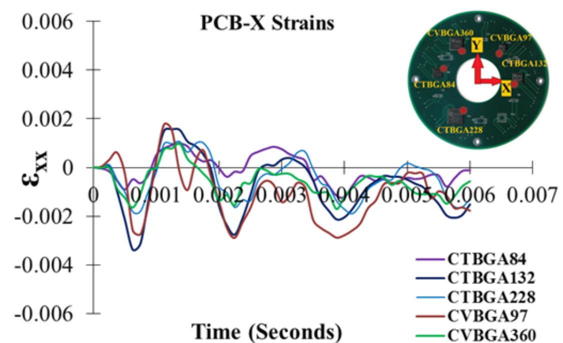

Figure 34: PCB-X strains of Armstrong A12 potted board @ 10,000g

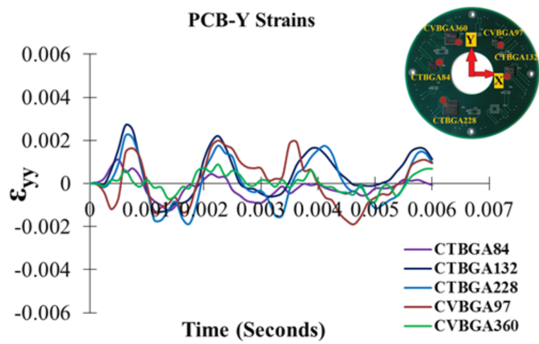

Figure 35: PCB-Y strains of Armstrong A12 potted board @ 10,000g

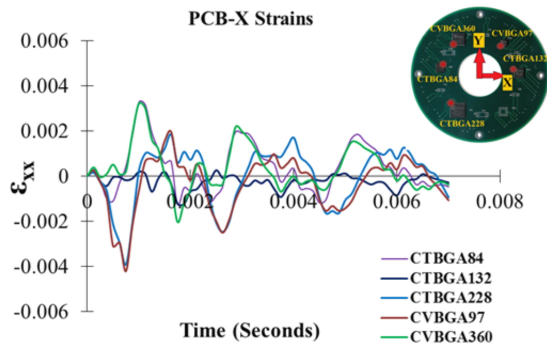

Figure 36: PCB-X strains of bare TV @ 25,000g shock

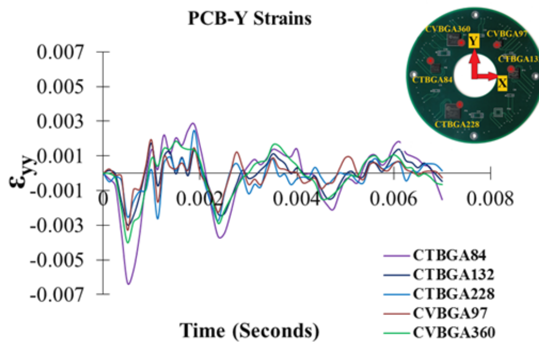

Figure 37: PCB-Y strains of bare TV @ 25,000g shock

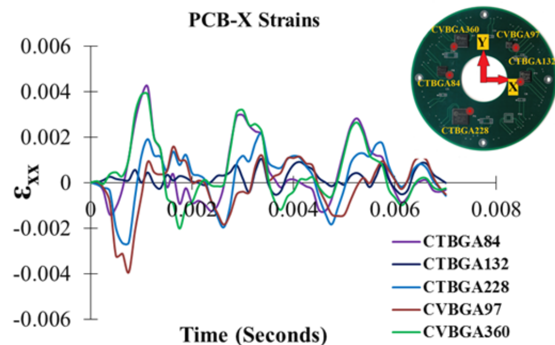

Figure 38: PCB-X strains of ME531 underfill reinforced TV @ 25,000g shock

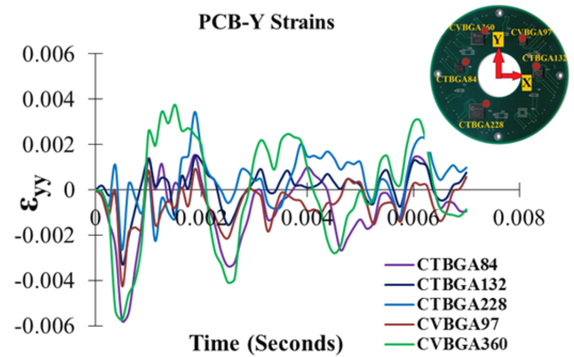

Figure 39: PCB-Y strains of ME531 underfill reinforced TV @ 25,000g shock

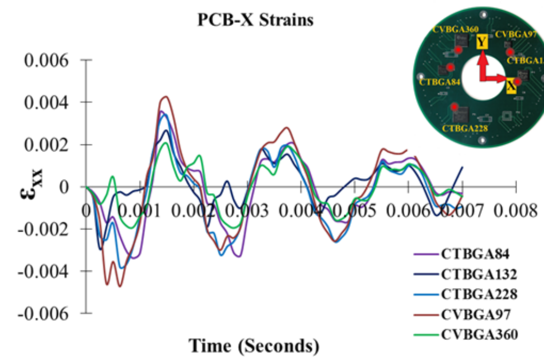

Figure 40: PCB-X Strains bare TV @50,000g

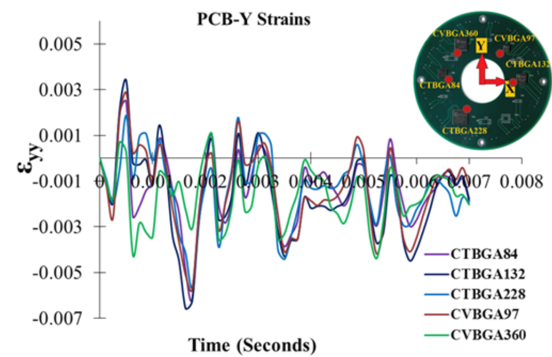

Figure 41: PCB-Y Strains bare TV @50,000g

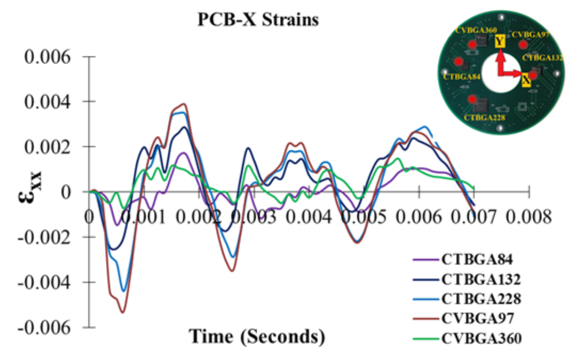

Figure 42: PCB-X strains of ME531 underfill reinforced TV @ 50,000g

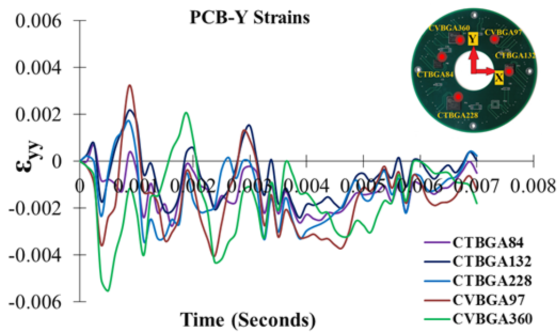

Figure 43: PCB-Y strains of ME531 underfill reinforced TV @ 50,000g

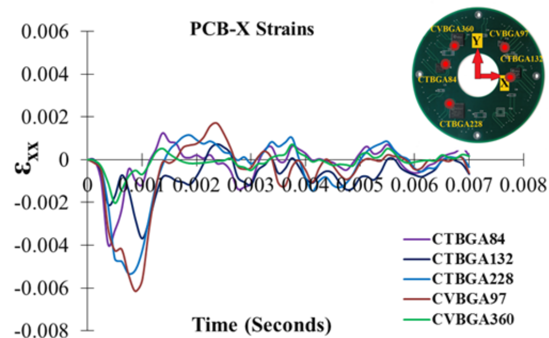

Figure 44: PCB-X strains of Armstrong A12 potted PCB @ 50,000g

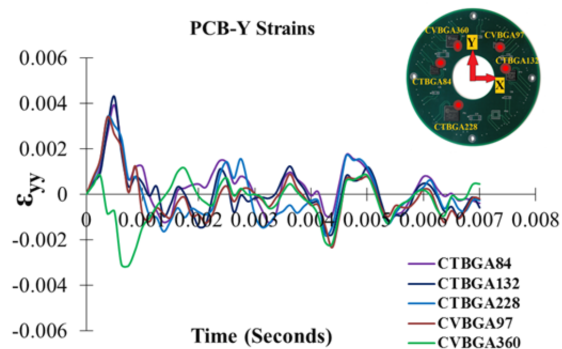

Figure 45: PCB-X strains of Armstrong A12 potted PCB @ 50,000g

Two components of the normal strain including x-strain and y-strain have been extracted for 5ms time-history after impact. For test assembly with STYCAST 2850FT potting material, Figure 32 and Figure 33 show pcb-x and pcb-y strains under 10,000g shock. The peak value near the corner interconnects of the packages were in the neighborhood of 4800με in pcb-x and 4100με in pcb-y. Similarly, Figure 34 and Figure 35 show the in-plane PCB strains of Armstrong A12 potted board subjected to 10,000g shock. Peak strains were 3300με in pcb-x and 2700με in pcb-y. Strain histories for x-strain and y-strain in unreinforced test assembly under 25,000g mechanical shock are shown in Figure 36 and Figure 37. Peak values of normal strain for 25,000g are 4200 με for pcb-x and 6800 με for pcb-y. Similarly, pcb-x and pcb-y strain histories for test assemblies with ME531 underfill are shown in Figure 38 and Figure 39. With ME531 underfill, the peak values of pcb-x and pcb-y in this case are 4300 με and 5600 με. In plane PCB strains at 50,000g for unreinforced bare TV is shown in Figure 40 and Figure 41. The peak values near the corner interconnects are in the neighborhood of 4500 με in x-direction and 6500 με in y-direction. Similarly the pcb-x and pcb-y strains at 50,000g for ME 531 underfill reinforced TV are shown in Figure 42 and Figure 43 respectively. Peak values near the marked corner regions are 5300 με in x and 5500 με in y. Figure 44 and Figure 45 show the in plane pcb-x and pcb-y strains of Armstrong A12 potted board subjected to 50,000g shock. The peak values are 6100 με in x and 4300 με in y can be seen from Figure 44 and Figure 45.

SURVIVABILITY AND FAILURE ANALYSIS

Survivability of the components under various package configurations at each G-level is discussed in this section. Figure 46 shows the survivability comparison of the four configurations of test board subjected to 10,000g shock. In the case of bare and underfill reinforced TVs CTBGA228 and CVBGA360 packages were the first ones to failure early just under 5 drops. These two packages are with bigger foot print compared to the rest. The underfill reinforced packages of CVBGA97, CTBGA84 and CTBGA132 survived at least 5-7 drops more as opposed to the bare TV condition at 10,000g shock. Contrasting results were observed between the two potting compounds STYCAST 2850FT and Armstrong A12. The total number of drops to fail all the components on the STYCAST 2850FT potted board at 10,000g shock is 6 with the earliest failure seen at 1st drop for CTBGA228, CVBGA97 and 6th drop for CTBGA132. The reason for the early failure of the components is attributed to the hard and brittle nature of the cured STYCAST 280FT epoxy.

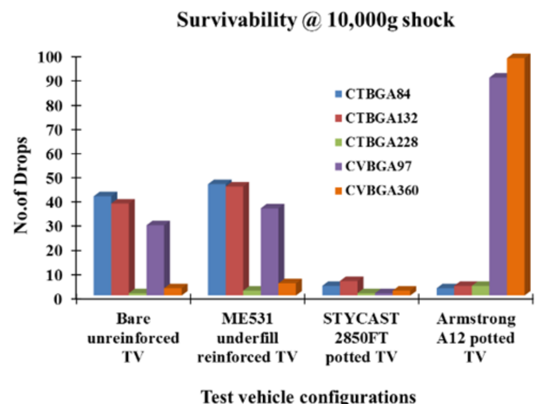

Figure 46: Survivability of various TV configurations @ 10,000g shock

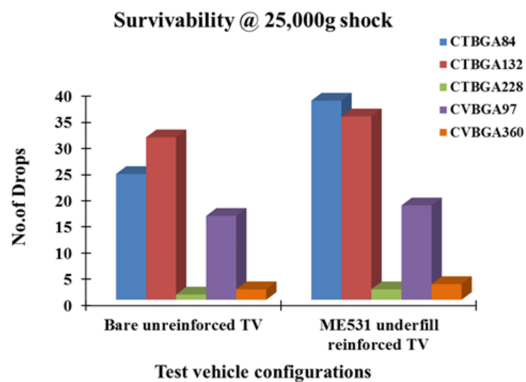

Figure 47: Survivability of various TV configurations @ 25,000g shock

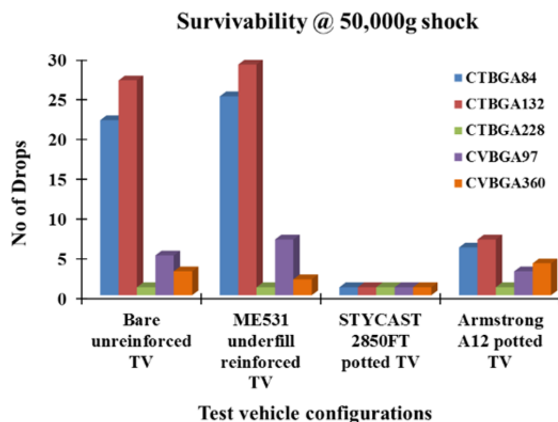

Figure 48: Survivability of various TV configurations @ 50,000g shock

During the progressive exposure of the test boards to drop the potting material fractured into pieces and peeled off from the board. The Armstrong A12 potting compound performed very well in mitigating the early failure of at least two packages CVBGA97 and CVBGA360 when compared to the STYCAST potted board. These CVBGA97 and CVBGA360 packages survived 90 and 98 drops with the Armstrong A12 potting compound respectively and the drop performance increased at least by 50 drops when compared to the Bare and underfill reinforced TVs. The in-plane PCB strains near the package corners of Armstrong A12 potted board were considerably less when compared to the STYCAST board @ 10,000g. Armstrong A12 excellently absorbed the shock and minimized the flexure which eventually increased drop performance. Unreinforced bare TV and ME531 underfill reinforced TV were subjected to 25,000g shock and the corresponding drops to failure chart is shown in Figure 47. CTBGA228 was the first package to fail under two drops in both conditions followed by CVBGA360 failing under five drops. Unreinforced bare TV package CTBGA132 survived maximum of 31 drops under 25,000g shock. When the G-level was increased from 10,000g to 25,000g the number of drops to failure decreased by 10 drops in the case of Bare TV. Similarly, in the case of ME531 underfill reinforced TV survivability has decreased by 8 drops. Figure 48 shows the survivability chart for the four package configurations subjected to 50,000g shock. CTBGA132 package survived maximum no. of drops in both Bare TV configuration and underfill TV at 50,000g shock which is 26 and 29 drops respectively. When compared to the 10,000g shock counter parts of the same test vehicle configuration the drop performance has decreased anywhere between 15-20 drops. In the case of potted boards STYCAST test vehicle followed the same trend failing all the components in the 1st drop itself. The potting compound shattered the same mode as seen the 10,000g shock case. All the packages in the Armstrong A12 potted board were also failed under 10 drops at 50,000g shock. The considerable decrease in the performance can be attributed to the inertial and high dynamic nature of the 50,000g ramp from 10,000g shock.

KALMAN FILTER FRAMEWORK FOR RUL

In functional electronics, there may be a number of noise sources. Often assessment of accrued damage and the assessment of remaining useful life must be done in the presence of measurement noise and process noise associated with the electronic system. In the present case, the damage progression in electronics subjected to high-g shock has been done using a Kalman Filter (KF). The Kalman Filter has been previously used in a number of applications including guidance and tracking [Kalman 1960, Zarchan 2000]. In the present case the damage in the electronic assemblies under high-g shock has been tracked using resistance measurement based state-vectors. A second order model has been used for damage tracking which includes resistance measurements from resistance spectroscopy, rate of change of resistance and the rate of change in time-gradient of resistance. The state vector is formulated at the beginning of the test with initialized values of process noise and measurement noise. The evolution of the state vector is modeled using a combination of system dynamics matrix, control matrix and the fundamental matrix in the presence of measurement noise and process noise. In each time step, the KF based model predicts the value of the state vector at the next time-step and computes the error with respect to the measured value. The KF gain evolves to reduce the error between the measured values of the state vector and the predicted value of the state vector. Once the error has dropped to an acceptable range, the KF model is used primarily in predictive mode for assessment of the remaining useful life. The process starts with control vector, u_k or input for the system in the presence of process noise, w_k. The state-vector at the kth time step, x_k is propagated in each time-step. The measurement matrix, H, maps the hidden variables into observable state variables, z_k in the presence of measurement noise, v_k. Each prediction step is undertaken after a time delay of T, using the system dynamics matrix Φ_k.

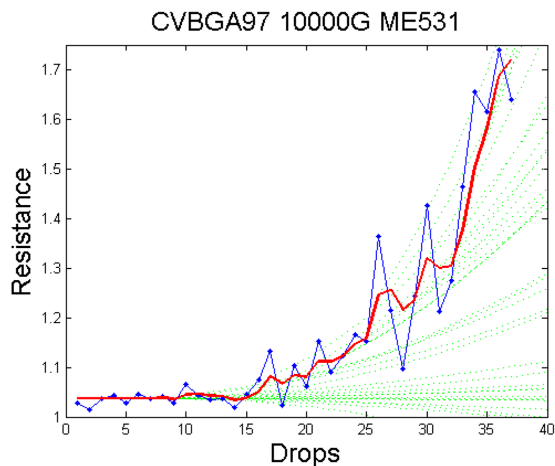

Figure 49: ME531 underfill reinforced CVBGA97 package resistance trend under 10000g shock

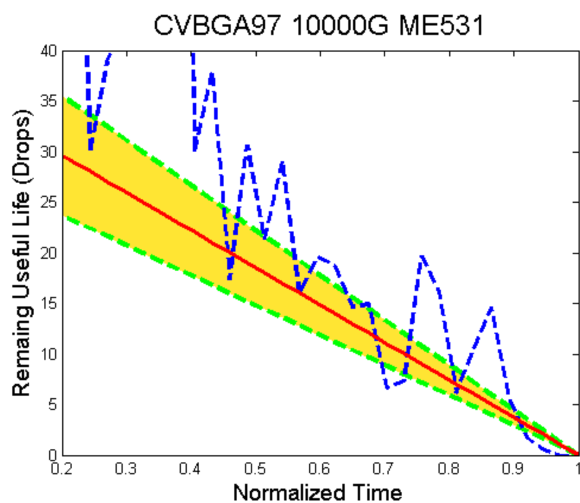

Figure 50: ME531 underfill reinforced CVBGA97 package remaining useful life prediction under 10000g shock.

The state-vector is predicted at each time step in the presence of measurement noise and process noise using the Kalman Filter equation:

$$\hat{x}_k = \Phi_k \hat{x}_{k-1} + B_k u_{k-1} + K_k \left(z_k - H_k \Phi_k \hat{x}_{k-1} - H_k B_k u_{k-1} \right) \quad (1)$$

$$z_k = H x_k + v_k \quad (2)$$

Where $\hat{x}_k$ is the Kalman Filter estimate of system-state at time k^{th} time step, and x_k is the actual system state at the kth time-step, B_k is the control vector. In order to model the system, a second order equation has been used to represent the system-state evolution resulting from the progression of underlying damage.

$$\begin{Bmatrix} \dot{x} \\ \ddot{x} \\ \dddot{x} \end{Bmatrix} = [F] \begin{Bmatrix} x \\ \dot{x} \\ \ddot{x} \end{Bmatrix} = \begin{pmatrix} 0 & 1 & 0 \\ 0 & 0 & 1 \\ 0 & 0 & 0 \end{pmatrix} \begin{Bmatrix} x \\ \dot{x} \\ \ddot{x} \end{Bmatrix} \quad (3)$$

Resistance spectroscopy based resistance measurements have been performed for each test condition between 10,000g-50,000g for all the components. Figure 49 shows the resistance readings of the package CVBGA97 of the underfilled TV under 10,000g shock condition. The resistance was seen to increase monotonically with the increase in exposure to shock-events, exponentially increasing after 25-drops. The remaining useful life (RUL) of the bare TV package for the CVBGA97 under 10,000g shock is shown in Figure 50.

SUMMARY AND CONCLUSIONS

Fine-pitch electronics for fuzing applications has been studied with high speed video in conjunction with 3D-DIC measurements for measurement of board strains under high-g mechanical shock. In addition, explicit finite element models have been used to study the transient dynamic behavior and predict the board strain and out of plane deformation of the assemblies. Model predictions have been used to extract the solder joint strains for g-levels in the neighborhood of 10,000g-50,000g in unreinforced, underfilled, and potted assemblies. Experimental data indicates that potting adds survivability margins for shock exposures upto 10,000g. However, for shock exposures higher than 10,000g the delamination failure mode between the potting compound and the printed circuit board dominates reducing the design margin. Underfilling of the electronic components added survivability margin at all g-levels. The highest I/O, fine-pitch components (CVBGA360, 0.4mm pitch; CTBGA228, 0.5mm pitch) in the study showed the poorest survivability in the study at all the g-levels studied. Kalman filter was able to track the damage accrued in shock-events accurately and prognosticate remaining useful life (RUL).

ACKNOWLEDGEMENTS

The research presented in this paper has been supported by NSF Center for Advanced Vehicle and Extreme Environment Electronics (CAVE3) consortium-members.

REFERENCES

Birzer, C., Bernd Rakow, Rainer Steiner, Juergen Walter "Drop Test Reliability Improvement of Lead-free Fine Pitch BGA Using Different Solder Ball Composition" Electronics Packaging Technology Conference, Singapore, Dec. 7-9, 2005

Chin, Y.T., P.K. Lam , H.K. Yow , T.Y. Tou , "Investigation of mechanical shock testing of lead-free SAC solder joints in fine pitch BGA package" Microelectronics Reliability, Vol. 48, pp. 1079–1086, 2008.

Constable J.H, Lizzul C, "An Investigation of Solder Joint Fatigue using Electrical Resistance Spectreoscopy" Components, Packaging, and Manufacturing Technology, Part A, IEEE Transactions on, Vol. 18, No. 1, pp. 142-152, 1995

Kalman, R., A New Approach to Linear Filtering and Prediction Problems, Transactions of the ASME--Journal of Basic Engineering, Vol. 82, No. D, pp. 35-45, 1960.

Lall, P., Patel, K., Lowe, R., Strickland, M., Blanche, J., Geist, D., Montgomery, R., Modeling and Reliability Characterization of Area-Array Electronics Subjected to High-G Mechanical Shock Up to 50,000G, Proceedings of the 62nd ECTC, pp. 1194 – 1204, May 29-June 1, 2012

Lall, P., Shantaran, S., Angral, A., Kulkarni, M., Explicit Submodeling and Digital Image Correlation Based Life-Prediction of Leadfree Electronics under Shock-Impact, Proceedings of 59th Electronic Components & Technology Conference, San Diego, California, pp. 542-555, May 25-29, 2009.

Lall, P., Iyengar, D., Shantaram, S., Pandher, R., Panchagade, D., Suhling, J., Design Envelopes and Optical Feature Extraction Techniques for Survivability of SnAg Leadfree Packaging Architectures under Shock and Vibration, Proceedings of the 58th Electronic Components and Technology Conference (ECTC), Orlando, Florida, pp. 1036-1047, May 27-30, 2008.

Lall, P. Panchagade, D., Liu, Y., Johnson, W., Suhling, J., Smeared Property Models for Shock-Impact Reliability of Area-Array Packages, ASME Journal of Electronic Packaging, Volume 129, pp. 373-381, December 2007[d].

Lall, P., Gupte, S., Choudhary, P., Suhling, J., Solder-Joint Reliability in Electronics Under Shock and Vibration using Explicit Finite Element Sub-modeling, IEEE Transactions on Electronic Packaging Manufacturing, Volume 30, No. 1, pp. 74-83, January 2007[b].

Lall, P., Panchagade, D., Iyengar, D., Shantaram, S., Suhling, J., Schrier, H., High Speed Digital Image Correlation for Transient-Shock Reliability of Electronics, Proceedings of the 57th ECTC, Reno, Nevada, pp. 924-939, May 29 – June 1, 2007.

Lall, P., Panchagade, D., Liu, Y., Johnson, R. W., and Suhling, J. C., Smeared-Property Models for Shock-Impact Reliability of Area-Array Packages, Journal of Electronic Packaging, Vol. 129(4), pp. 373-381, 2007.

Lall, P., Dhananjay R. Panchagade, Yueli Liu, R. Wayne Johnson,Jeffrey C. Suhling, "Models for Reliability Prediction of Fine-Pitch BGAs and CSPs in Shock and Drop-Impact" IEEE Transactions On Components And Packaging Technologies Vol. 29, No. 3, September 2006

Tian, G., Y Liu, RW Johnson, P Lall, M Palmer, MN Islam, L Crane, Corner bonding of CSPs: processing and reliability, Electronics Packaging Manufacturing, IEEE Transactions on 28 (3), 231-240, 2005.

Xu, L., Pang, H., Combined Thermal and Electromigration Exposure Effect on SnAgCu BGA Solder Joint Reliability, Electronic Components and Technology Conference, pp. 1154-1159, May 2006.

Yogel, D., Grosser, V., Schubert, A., Michel, B., MicroDAC Strain Measurement for Electronics Packaging Structures, Optics and Lasers in Engineering, Vol. 36, pp. 195-211, 2001.

Zarchan, P., and H. Musoff, Fundamentals of Kalman Filtering: A Practical Approach, Vol. 190. Progress in Astronautics and Aeronautics, American Institute of Aeronautics and Astronautics (AIAA), 2000.

Zhang, F., Li, M., Xiong, C., Fang, F., Yi, S., Thermal Deformation Analysis of BGA Package by Digital Image Correlation Technique, Microelectronics International, Vol.22, No. 1, pp. 34-42, 2005.

Zhou, P., Goodson, K. E., Sub-pixel Displacement and Deformation Gradient Measurement Using Digital Image- Speckle Correlation (DISC), Optical Engineering, Vol. 40, No. 8, pp 1613-1620, August 2001.